

Algorithms underlying flexible phototaxis in larval zebrafish

Alex B. Chen^{1,2,3,‡}, Diptodip Deb³, Armin Bahl^{1,*} and Florian Engert¹

ABSTRACT

To thrive, organisms must maintain physiological and environmental variables in suitable ranges. Given that these variables undergo constant fluctuations over varying time scales, how do biological control systems maintain control over these values? We explored this question in the context of phototactic behavior in larval zebrafish. We demonstrate that larval zebrafish use phototaxis to maintain environmental luminance at a set point, that the value of this set point fluctuates on a time scale of seconds when environmental luminance changes, and that it is determined by calculating the mean input across both sides of the visual field. These results expand on previous studies of flexible phototaxis in larval zebrafish; they suggest that larval zebrafish exert homeostatic control over the luminance of their surroundings, and that feedback from the surroundings drives allostatic changes to the luminance set point. As such, we describe a novel behavioral algorithm with which larval zebrafish exert control over a sensory variable.

KEY WORDS: Larval zebrafish, Phototaxis, Homeostasis, Allostatic control, Luminance adaptation, Behavioral tracking

INTRODUCTION

All living organisms exert control over a variety of physiological variables. For example, animals employ sophisticated control systems to keep body temperature, body mass, blood osmolarity and many other parameters within narrow ranges critical for bodily function (Cannon, 1939). Many of these homeostatic processes involve comparing moment-to-moment values of the controlled physiological variables with ‘set points’ that the control system seeks to maintain. When a variable deviates from its set point, the control system acts, often via negative feedback, to restore the variable to its set value.

Conceptualizations of homeostatic control often treat set points as fixed in value, but changing environmental or internal conditions could render an existing, fixed, set point maladaptive (Woods and Ramsay, 2007). When this occurs, a robust control system ought to flexibly adjust its set point to a range adaptive to the new conditions. This process has been termed allostasis (Morville et al., 2018 preprint; Sterling, 2012), and allostatic shifts in set points occur everywhere across the animal kingdom. For example, many endothermic animals exhibit an elevated body temperature set point, fever, in response to infection (Cabanac and Massonnet, 1974; Moltz, 1993), whereas animals that hibernate through the

winter reduce their body temperature set point during hibernation, but increase their caloric set point before hibernation sets in (Mrosovsky and Fisher, 1970; Ortmann and Heldmaier, 2000). Finally, homeostatic and allostatic control can involve behavioral, in addition to physiological, changes. Ectothermic animals that regulate body temperature by seeking out warmer or cooler regions of the environment also exhibit behavioral fever (Rakus et al., 2017). Despite the ubiquity of allostasis in physiology, it is still poorly understood how physiological control systems adjust their set points in response to changing internal and external conditions, and how allostasis interacts with homeostatic control.

In this study, we establish luminance-based navigation in larval zebrafish as a model for investigating behavioral allostatic control. Previous work on luminance-based navigation in larval zebrafish has focused on their tendency to orient and swim towards brighter regions of luminance gradients; this behavior is termed positive phototaxis (Brockerhoff et al., 1995; Chen and Engert, 2014; Chen et al., 2018; Guggiana-Nilo and Engert, 2016; Karpenko et al., 2020; Wolf et al., 2017). However, in naturalistic environments, luminance varies widely, both throughout the day and as fish move into and out of shade. Therefore, a strategy of purely positive phototaxis might not be adaptive to larval zebrafish, and it is likely too simplistic a view of this complex behavior. Indeed, evidence of flexibility in the phototactic behavior of larval zebrafish has been documented. One study demonstrated that larval zebrafish avoid light sources that are too bright and that this avoidance depends on the luminance to which fish are pre-adapted (Burgess et al., 2010). Another study revealed that larval zebrafish exhibit negative phototaxis in gradients of near-infrared light (Hartmann et al., 2018). These findings suggest that the phototactic behavior of larval zebrafish is flexible and can be modulated by environmental luminance and its history.

We sought to characterize the behavioral algorithms that underlie the flexibility of phototaxis in larval zebrafish. Towards that end, we delivered closed-loop luminance gradient stimuli to freely swimming larval zebrafish that were pre-adapted to different luminance histories, and we formulated simple behavioral algorithms that could explain the resultant behavior. We found that larval zebrafish perform positive and negative phototaxis to orient towards a set point luminance, the value of which depends on the luminance history of their surroundings. Furthermore, fish compute the set point luminance using visual information from both eyes. These findings uncovered previously unappreciated principles underlying phototaxis in larval zebrafish, namely that the larval zebrafish employs phototaxis to maintain its experienced luminance at a fixed value and that its luminance preference fluctuates in response to changing environmental luminance conditions. We believe that this behavioral control of experienced luminance can serve as a model for investigating neural implementations of homeostatic and allostatic control.

MATERIALS AND METHODS

Experimental model and subject details

Experiments were conducted according to the guidelines of the National Institutes of Health and were approved by the Standing

¹Department of Molecular and Cellular Biology, Harvard University, Cambridge, MA 02138, USA. ²Program in Neuroscience, Harvard Medical School, Boston, MA 02115, USA. ³Janelia Research Campus, Howard Hughes Medical Institute, Ashburn, VA 20147, USA.

*Present address: Centre for the Advanced Study of Collective Behaviour, University of Konstanz, 78464 Konstanz, Germany.

[‡]Author for correspondence (abchen@g.harvard.edu)

 A.B.C., 0000-0003-3950-4460; A.B., 0000-0001-7591-5860

Committee on the Use of Animals in Research of Harvard University. Animals were handled according IACUC protocol #2729. For all experiments, we used wild-type larval zebrafish (strains AB and WIK), aged 5–8 days post-fertilization (dpf). We did not determine the sex of the fish we used. Fish were raised in shallow Petri dishes and fed *ad libitum* with paramecia after 4 dpf. Fish were raised on a 14 h:10 h light:dark cycle at around 27°C. All experiments were done during daylight hours (4–14 h after lights on). All protocols and procedures were approved by the Harvard University/Faculty of Arts and Sciences Standing Committee on the

Use of Animals in Research and Teaching (Institutional Animal Care and Use Committee).

Method details

Design of system for tracking and closed-loop video projection

For behavioral experiments related to Figs 1–3, we used the same behavioral system for tracking freely swimming larval zebrafish as in Bahl and Engert (2020). Larval zebrafish swam freely in custom-made, circular, acrylic dishes with black walls and filled with filtered system water. Dish diameter was 12 cm; wall height was

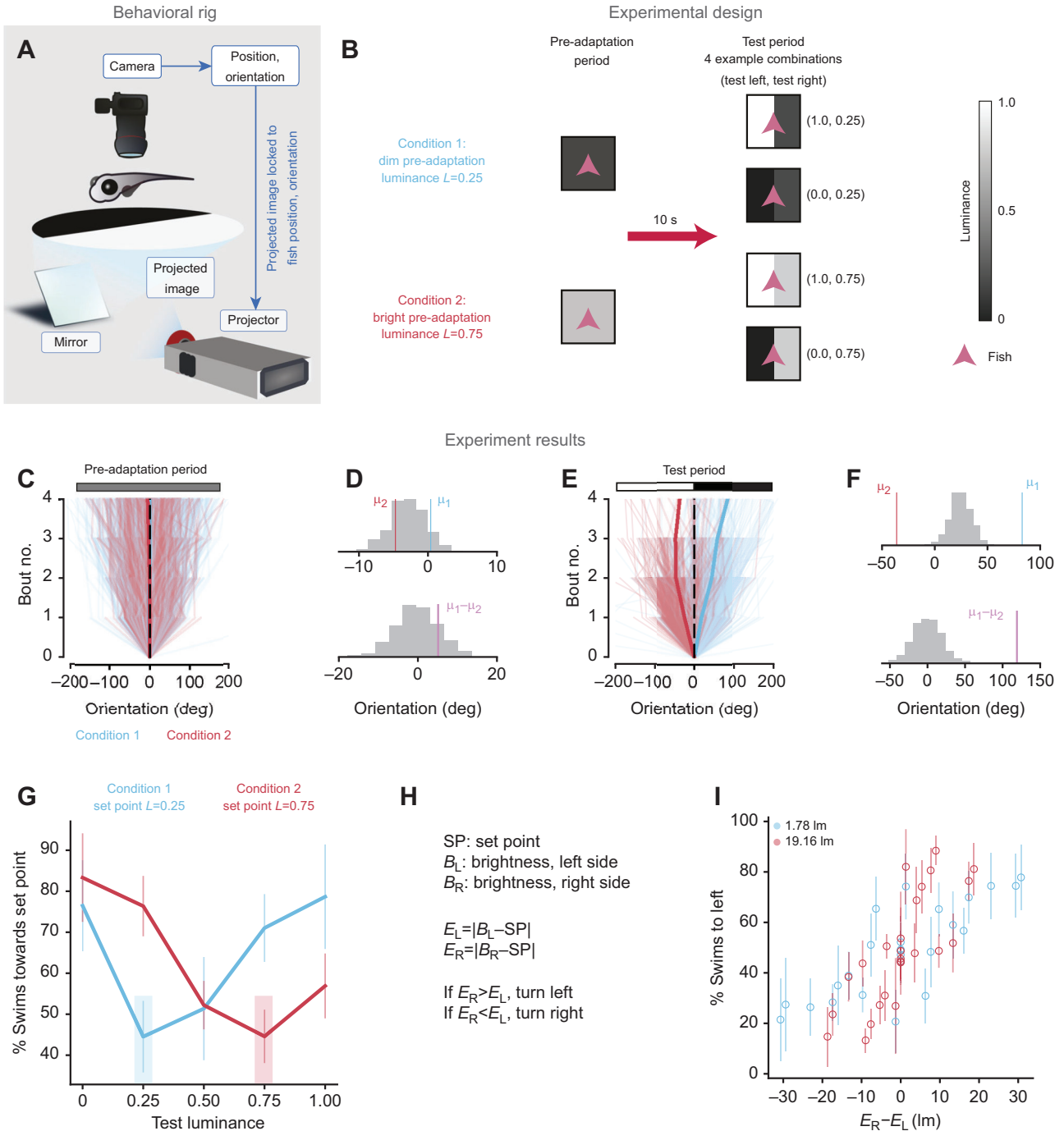


Fig. 1. See next page for legend.

Fig. 1. Larval zebrafish orient towards a set point during luminance-based navigation.

(A) Schematic diagram of the experimental setup. Larval zebrafish swim freely while visual stimuli are presented locked to fish reference frames (see Materials and Methods). (B) Experimental design. Each trial consisted of two periods. During the first period ('pre-adaptation') fish were held in a dim ($L=0.25$, $n=11$ fish) or bright ($L=0.75$, $n=8$ fish) environment for at least 10 s. Immediately following pre-adaptation, fish were subjected to a test period for at least 3 s. During the test period, the left and right sides of the environment relative to the fish were held at brightness values (B_L , B_R) selected pseudo-randomly from the set {0, 0.25, 0.50, 0.75, 1.00}. (C) Change in orientation of fish over the last 3 s of pre-adaptation. The color bar reflects equal luminance on the two sides of the fish. Each trace shows the change in orientation in a single trial for a single animal. Orientation values are presented relative to the animal's orientation 3 s before test period onset. Blue traces: condition 1 ($n=11$ fish, 2200 trials). Red traces: condition 2 ($n=8$ fish, 720 trials). Thicker traces show the mean of each condition (partial overlap with dashed line). (D) Statistical comparison between pre-adaptation periods in conditions 1 and 2. Top: gray histogram shows bootstrapped distribution of trials shuffled randomly and split with 2200 trials in one group and 720 in another to preserve group size (1000 bootstrapped means). Red and blue ticks show observed means for conditions 1 and 2, respectively ($\mu_1=0.40$ deg, $\mu_2=-4.72$ deg); they fall within the 90% confidence interval (CI) of the shuffled mean [-7.31 deg, 1.26 deg]. Bottom: the bootstrapped null distribution of the difference in means between the two conditions (1000 bootstrapped differences). Trials were shuffled and sorted as described for the histogram above. The purple tick shows the observed difference in means ($\mu_1-\mu_2=5.12$ deg), which falls within the 80% CI of the shuffled difference [-7.25 deg, 6.89 deg]. (E) Same as C for the test period. Negative orientation angles were defined to be in the bright direction and positive orientation angles were defined to be in the dim direction, as shown in the color bar. Note the clear separation between the two conditions. (F) Same as D for the test period. Observed means and difference between means fall completely outside bootstrapped distributions for shuffled data (1000 bootstrapped values for each distribution), indicating a difference significant to $P<0.001$. (G) Analysis of the test period for trials in which one side of the fish was at set point luminance. The luminance of the other side was considered the test luminance. The shaded region denotes the set point luminance. Bias towards the set point side depended significantly on the test luminance (ANOVA, d.f.=4, $P<0.05$ for both conditions): bias towards the set point luminance was higher when the test luminance deviated from the set point than when the test luminance was equal to the set point luminance (condition 1: test luminance 0.25 versus test luminance 1.0, t -test $P<0.01$; condition 2: test luminance 0.75 versus test luminance 0.0, t -test $P<0.01$). Error bars denote standard deviation across fish. (H) Explanation of abbreviations and calculations used to generate I. (I) Percentage of leftward swims plotted as a function of relative distance from the set point: E_R-E_L . Higher E_R-E_L values drive higher leftward swim bias (t -test on slope of linear fit, $P<0.001$). Error bars denote standard deviation across fish.

5 mm. Fish were bottom-lit using light-emitting diode (LED) arrays (940 nm, Cop Security) so that the shadow they cast could be used to determine their position and orientation. We tracked the fish using a Grasshopper3-NIR camera (FLIR Systems) equipped with a zoom lens (Zoom 7000, 18–108 mm, Navitar) and a long-pass filter (R72, Hoya). Frame data were stably acquired at around 90 frames s^{-1} and analyzed in real time to extract fish position and orientation. For each experiment, we used two groups of four cameras, with each group of four connected to a different computer; thus, each computer could track four separate fish simultaneously. Fish were tracked using code written in C++, Python 3.7 and OpenCV 4.1 (see 'Quantification and statistical analysis', below). We delivered visual stimuli locked to the position and orientation of the fish.

Visual stimuli

We delivered different luminance values to the fish by commanding a video projector (60 Hz, AAXA P300 Pico Projector) to project different grayscale pixel values, ranging from 0 (black) to 1 (white). We used an iPhone 11 Pro and the Lux Light Meter Pro app at a distance of about 5 cm above the dish to measure brightness levels: $L=0$

(0.46 lm), $L=0.25$ (1.78 lm), $L=0.5$ (9.42 lm), $L=0.75$ (19.16 lm), $L=1$ (32.49 lm) (Fig. S1A). Visual stimuli were projected from below onto white paper to disperse the light for visibility. Visual stimuli were projected in the reference frame of the fish. For split-luminance experiments, all pixels with negative x values in this coordinate system were defined to be left of the fish, and all pixels with positive x values were defined to be right of the fish. For all experiments, following the probe period, fish experienced the same luminance conditions as in the pre-adaptation period for at least 10 s. After this, the next trial began. For the experiments in Fig. 1, we included mirror symmetric controls (Fig. S2A).

Set point seeking experiments

As shown in Fig. 1, we held the fish in either dim ($L=0.25$) or bright ($L=0.75$) luminance for 10 s, and then subjected it to a split-luminance test period in which the luminance of the left and right sides of the fish was selected randomly from five possible pixel values (0, 0.25, 0.5, 0.75, 1). For the bright pre-adaptation experiments, the test period lasted for 10 s; however, we noticed a decrease in turning bias after the first few seconds due to adaptation (Fig. S2E,F). As a result, we limited the test period to 3 s for the dim pre-adaptation experiments and only analyzed the first 3 s of the test period in both conditions.

Split-luminance pre-adaptation experiments

As shown in Fig. 2, we held the fish in a split-luminance environment (luminance on dim side: $L=0$; luminance on bright side: $L=1$) for 16 s. After this pre-adaptation period, we changed the luminance of either the bright side or the dim side for 10 s.

Two pre-adaptation experiments

As shown in Fig. 3, we held the fish in an initial pre-adaptation period ($L=0.25$ or $L=0.75$) for 16 s. We then held the fish in a second pre-adaptation period; if the luminance during the initial pre-adaptation was $L=0.25$, the luminance during the second pre-adaptation was $L=0.75$. Conversely, if the luminance during the initial pre-adaptation was $L=0.75$, the luminance during the second pre-adaptation was $L=0.25$. Across different trials, the length of the second pre-adaptation period was chosen pseudorandomly from these possible values: 0 s (i.e. no second pre-adaptation), 3, 6, 9 and 12 s.

Modeling

Complete details on our *in silico* experiment settings and initializations of fish parameters are available on GitHub at <https://github.com/diptodip/brightfish>.

We simulated two computational models of zebrafish phototaxis: one using separate monocular information and one integrating binocular information. All simulations occurred within a 2D grid of dimensions (H, W) (rows, columns). In our simulations, both height (H) and width (W)=101 for the spotlight experiment (Fig. 4G) and H and W=51 for the partitioned halves experiments (Figs 2 and 4D). We simulated fish as points without volume within this grid. For both models, the fish calculates brightness in each eye as the mean value of all grid tiles falling within two coterminal rays originating from the fish position with an angle of 0.8π between them.

At each time step, the simulated fish first updates its set point(s). The monocular fish has two set points, one for the left eye (SP_L) and one for the right eye (SP_R). It will calculate the differences:

$$\Delta SP_L = SP_L - B_L, \quad (1)$$

$$\Delta SP_R = SP_R - B_R, \quad (2)$$

where B_L and B_R are brightness values experienced by the left and right eye, respectively, and then use a learning rate r to update its set

points:

$$SP_{L,i} = SP_{L,i-1} - r \times \Delta SP_L, \quad (3)$$

$$SP_{R,i} = SP_{R,i-1} - r \times \Delta SP_R. \quad (4)$$

The binocular fish has one set point. It will calculate the difference:

$$\Delta SP = SP - 0.5(B_L + B_R). \quad (5)$$

And similarly use the learning rate to update the set point:

$$SP_i = SP_{i-1} - r \times \Delta SP. \quad (6)$$

After updating its set point(s), the fish turns in the direction of the eye with a smaller difference from the set point as described in Results; if the difference between the error signals from the left and right sides $E_L - E_R > 0$, the fish turns right; otherwise, the fish turns left. The fish samples a turn angle from one of two normal (N) distributions – one from the no-turn distribution $\Delta\theta_n \sim N(0.01, 0.50)$ and the other from the turn distribution $\Delta\theta_t \sim N(0.52, 0.59)$. The choice of distribution is given by a binomial with probability of choosing the turn distribution $f(E_L - E_R)$, where f is a non-linear function $f(x) = c|x|^{1/3}$, $x \in [-1, 1]$, and c is maximum turn probability (we use $c=0.75$). The non-linearity f and maximum turn probability c are included to better map $E_L - E_R$ to the turn behavior of real fish. The choice of exponent in f does not greatly affect fish behavior (data not shown). The sign of the turn direction is flipped for right turns versus left turns and we describe angles in radians. These distributions were generated by fitting Gaussian curves to turn angle distributions of the pre-adaptation period (no-turn distribution) or test period (turn distribution) of the condition in Fig. 1 where pre-adaptation luminance was 0.75 and the test period luminances were (0.75, 0) (data available from GitHub: <https://github.com/diptodip/brightfish/tree/master/experiments>). Then, the fish updates its heading as $\theta = (\theta + \Delta\theta) \bmod 2\pi$. Finally, the fish determines whether a swim occurs at this time step by sampling from a Bernoulli distribution with probability p_{move} . If the fish swims at this time step, it samples a move distance $d \sim N(\mu_d, \sigma_d)$ and moves d units in its heading direction θ . We used a learning rate r of 0.001, a p_{move} of 0.2, and a move distance distribution $d \sim N(5.0, 1.0)$, chosen to roughly match fish swim/set point adjustment behavior within our arbitrary space and time coordinate space.

Quantification and statistical analysis

Closed-loop tracking and swim-bout detection for freely swimming zebrafish

Software used for tracking freely swimming larval zebrafish and detecting swim bouts in real time was the same as in Bahl and Engert (2020). First, the image background was calculated as the mode image over approximately 60 s. For each acquired image frame, the background was subtracted. In the mode-subtracted image, the center of mass was defined to be the position of the larval zebrafish, and we used second-order image moments to determine its orientation. To detect swim bouts, we calculated a variance over a rolling, 50 ms time window. Variance spikes, subject to interbout interval constraints, were used to determine swim bout times.

Statistical tests

Details of statistical tests used in this study can be found in the figure legends. Unless otherwise specified in the figure legends, error bars signify \pm s.d. around the mean. Trials were selected pseudorandomly using the output of a random number generator and without human input. Sample sizes were not predetermined. We excluded fish that appeared for long periods in the image background, as this

suggested that they were dead or otherwise immobile. All exclusion was done prior to data analysis.

RESULTS

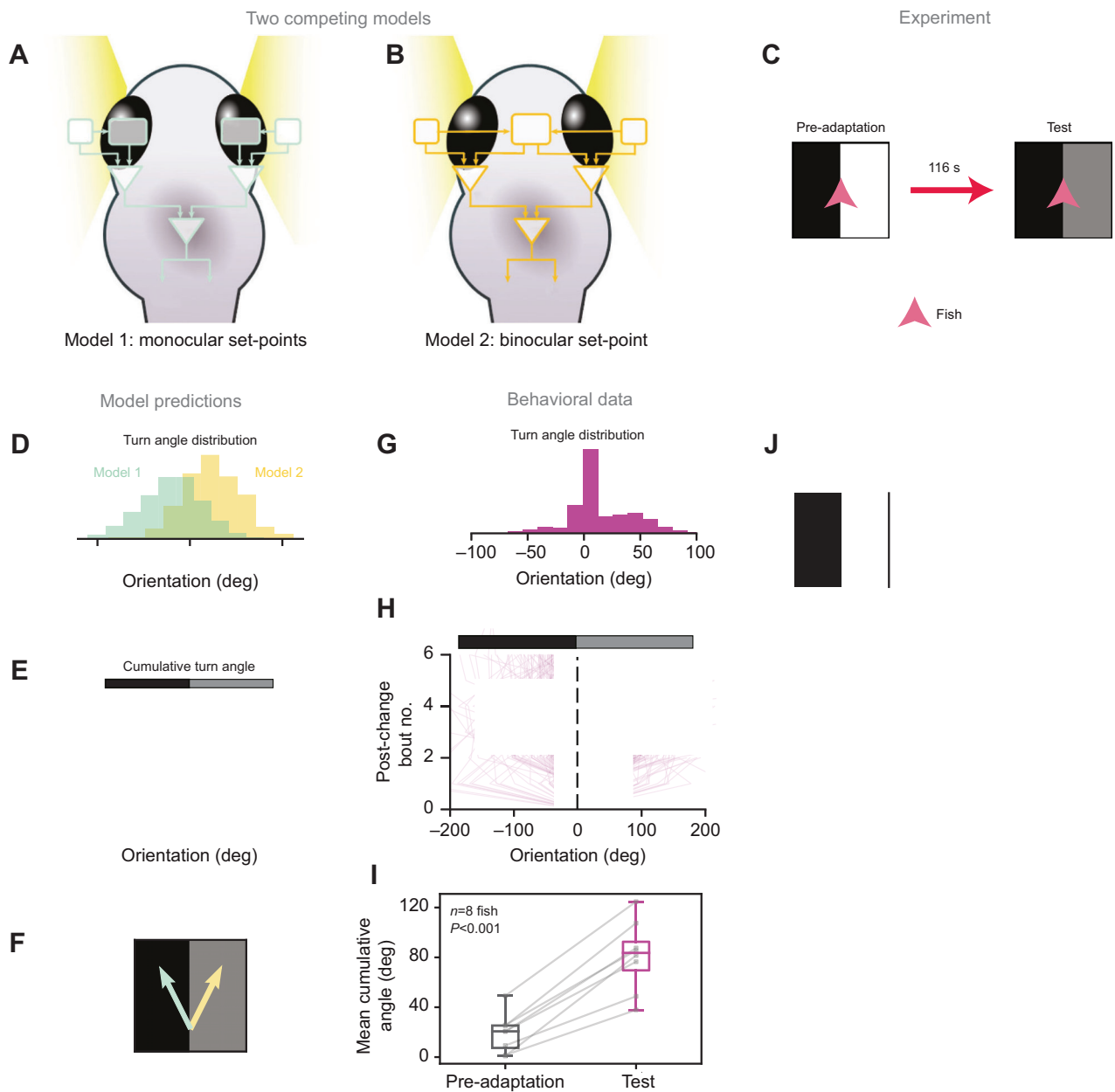
Larval zebrafish orient towards a set point during luminance-based navigation

To deliver controlled luminance stimuli to freely swimming larval zebrafish (5–8 dpf), we employed a closed-loop video projection system (Fig. 1A) used in previous work (Bahl and Engert, 2020) (see Materials and Methods). Here, a high-speed camera recorded a video of a fish swimming in a shallow, circular dish, a computer-vision program then calculated its position and orientation in real time, and a projector used this information to deliver visual stimuli fixed to the fish's reference frame. As a result, the visual stimuli, and in particular a specific luminance, could be kept constant on the fish's eyes, even if the animal moved continuously through the arena (see Materials and Methods).

Larval zebrafish were pre-adapted to either a bright ($L=0.75$, see Materials and Methods) or a dim ($L=0.25$) luminance level for 10 s (Fig. 1B, pre-adaptation period). The following pixel gray-scale values and their respective luminance values were used: $L=0$ (0.46 lm), $L=0.25$ (1.78 lm), $L=0.5$ (9.42 lm), $L=0.75$ (19.16 lm) and $L=1$ (32.49 lm) (Fig. S1A). To allow for comparison with other work (Burgess et al., 2010), we estimated the intensity of our illuminations using a luminous efficacy of 90 lm W^{-1} to yield $45 \mu\text{W cm}^{-2}$ at $L=0$ and 3.2 mW cm^{-2} at $L=1$. Following this pre-adaptation period, the fish experienced a split-luminance environment: a test period in which one visual hemifield was bright ($L=1$) and the other visual hemifield was dim ($L=0$) (Fig. 1B). We included a mirror-symmetric control for all stimuli used in Fig. 1 (Fig. S2A). As shown in previous work (Colwill and Creton, 2011; Dunn et al., 2016; Fero et al., 2011; Huang et al., 2013; Johnson et al., 2020; Marques et al., 2018), during the pre-adaptation period, when fish experienced uniform luminance, we observed no significant bias in turn direction (Fig. 1C,D).

However, a comparison of the swimming statistics during the pre-adaptation period (Fig. 1C,D) and the test period (Fig. 1E,F) revealed that fish do not simply perform positive phototaxis, as has been suggested by previous studies (Brockerhoff et al., 1995; Guggiana-Nilo and Engert, 2016; Karpenko et al., 2020; Wolf et al., 2017); instead, they consistently turned towards the side closest in luminance to that in the pre-adaptation period. This indicates that larval zebrafish prefer a luminance similar to the pre-adaptation luminance, suggesting that this value serves as a set point for subsequent luminance-driven navigation. Thus, fish pre-adapted to a bright environment exhibited a turning bias towards the bright visual hemifield during the test period, while fish pre-adapted to a dim environment exhibited a turning bias towards the dim visual hemifield during the test period (Fig. 1E,F; Fig. S2D). The turning bias was highest immediately after switching from the pre-adaptation period to the test period, and gradually declined throughout the test period (Fig. S2E,F). To limit the effect of this adaptation on our analyses, we considered turning behavior only within the first 3 s of the test period for the analyses presented in Fig. 1. In addition, we examined whether there were differences in other bout statistics between the different pre-adaptation conditions (Fig. S2B,C). We found no difference in the latency to the first bout but saw a transient elevation in bout rate following the transition from the dim pre-adaptation to the test period.

If the pre-adaptation luminance is truly the luminance set point during the test period, then fish should prefer the pre-adaptation luminance to any other luminance. To investigate this, we held one



visual hemifield constant at the pre-adaptation luminance during the test period and changed the luminance of the other hemifield over a large range of luminances ($L=0, 0.25, 0.5, 0.75$ and 1). To normalize differences in the number of swim bouts across different trials, we

calculated the percentage of leftward swims (defined to be negative angles) and rightward swims (positive angles) for each trial. This measure corresponded well with the accumulated angle measure used in Fig. 1C–F (Fig. S2G). We next tested a large set of

ERROR: stackunderflow
OFFENDING COMMAND: moveto

STACK: